J Physiol 589.7 (2011) pp 1707–1724

The Journal of Physiology

Minimal alterations in T-type calcium channel gating markedly modify physiological firing dynamics

A. Tscherter[1,2], F. David[1,2], T. Ivanova[1,2], C. Deleuze[3], J. J. Renger[4], V. N. Uebele[4], H-S. Shin[5], T. Bal[3], N. Leresche[1,2] and R. C. Lambert[1,2]

[1] *UPMC Univ Paris 6, France*
[2] *CNRS, UMR 7102, Paris, France*
[3] *UNIC CNRS UPR 3293, Gif-sur-Yvette, France*
[4] *Merck Research Laboratories, West Point, PA, USA*
[5] *Center for Neural Science, Korea Institute of Science and Technology, Seoul, Korea*

Non-technical summary Voltage-dependant calcium channels constitute a heterogeneous group playing ubiquitous roles in excitable cells. Among them the low-voltage activated T-type channels generate a family of currents that differ in their biophysical properties reflecting structural or neuromodulatory diversity. These T-type calcium channels are highly expressed in neurons located in the thalamus, a brain structure considered as the gateway to the cortex. Thalamic T-type calcium channels are critically involved in oscillatory neuronal activities associated with sleep or epilepsy and may contribute to sensory processing. Using injections of computer-simulated T-type conductances (a real time mimicry of ionic currents) in biological thalamic neurons, we dissect how the diversity in T-type currents impact on the output of thalamic neurons. We show that very subtle modifications in the properties of the T current that were overlooked so far affect drastically the physiological output of the thalamic neurons and therefore condition the dynamics of thalamo-cortical information integration.

Abstract T-type calcium channel isoforms expressed in heterologous systems demonstrate marked differences in the biophysical properties of the resulting calcium currents. Such heterogeneity in gating behaviour not only reflects structural differences but is also observed following the regulation of channel activity by a number of ligands. However, the physiological impact of these differences in gating parameters of the T channels has never been evaluated *in situ* where the unique interplay between T-type calcium and other intrinsic currents is conserved, and T channel activation can be triggered by synaptic stimulation. Here, using the dynamic clamp technique, artificial T conductances were re-incorporated in thalamic neurons devoid of endogenous T currents to dissect the physiological role of the T current gating diversity on neuronal excitability. We demonstrate that the specific kinetics of the T currents in thalamocortical and nucleus reticularis thalami neurons determine the characteristic firing patterns of these neurons. We show that subtle modifications in T channel gating that are at the limit of the resolution achieved in classical biophysical studies in heterologous expression systems have profound consequences for synaptically evoked firing dynamics in native neurons. Moreover, we demonstrate that the biophysical properties of the T current in the voltage region corresponding to the foot of the activation and inactivation curves drastically condition physiologically evoked burst firing with a high degree of synaptic input specificity.

(Received 10 December 2010; accepted after revision 8 February 2011; first published online 14 February 2011)
Corresponding author R. C. Lambert: UPMC Université Paris 6, UMR 7102 CNRS, Paris, France. Email: regis.lambert@snv.jussieu.fr

Abbreviations AP, action potential; G_{IT}, T conductance; ISI, inter-spike-interval; IT_a, artificial calcium T current; LTS, low threshold calcium spike; NRT, nucleus reticularis thalami; TC, thalamocortical; VB, ventrobasal nucleus.

DOI: 10.1113/jphysiol.2010.203836

Introduction

T-type Ca^{2+} channels, characterized by their low voltage of activation and their nearly complete inactivation at resting membrane potentials, generate transient currents with amplitudes that could reached several nanoamps in thalamic neurons (Crunelli *et al.* 1989; Leresche *et al.* 2004). These large currents are responsible for the slow depolarizing waveform called the low threshold calcium spike (LTS) that supports high-frequency firing in a number of different neuronal populations (Llinas & Yarom, 1981; Llinas & Jahnsen, 1982; Jahnsen & Llinas, 1984; Llinas & Muhlethaler, 1988). Molecular cloning and expression studies have established the existence of three genes coding for the Cav3.1, 2 and 3 isoforms of the T channels with multiple splice variants (Perez-Reyes, 2003). Investigations in heterologous expression system have demonstrated marked differences in the biophysical properties of these isoforms (Klockner *et al.* 1999; Kozlov *et al.* 1999; Monteil *et al.* 2000*a*,*b*; Chemin *et al.* 2001*a*,*b*; Murbartian *et al.* 2002, 2004; Emerick *et al.* 2006; Powell *et al.* 2009) and pronounced effects on their gating properties by a number of ligands such as glutamate, redox agents (e.g. ascorbate), signalling molecules (e.g. Zn^{2+}) and bioactive lipids (e.g. anandamide) (Chemin *et al.* 2001*a*, 2007; Nelson *et al.* 2005; Cataldi *et al.* 2007; Traboulsie *et al.* 2007; Hildebrand *et al.* 2009). However, the direct physiological impact of such heterogeneity of gating parameters of the T channels has never been evaluated *in situ* where native channel isoforms are present, the unique interplay between T current and the other intrinsic currents is conserved, and T channel activation can be triggered by physiological stimuli.

Here, the dynamic-clamp method was used to re-incorporate artificial T conductances with different properties in thalamic neurons devoid of endogenous T currents (Kim *et al.* 2001; Dreyfus *et al.* 2010). Using this approach, we demonstrate that the very large depolarizing T current and its specific kinetics are fully responsible for the high-frequency reached during burst firing in both thalamocortical (TC) neurons and the GABAergic neurons from the nucleus reticularis thalami (NRT), and that they determine their characteristic firing patterns. Moreover, we show that even minor alterations in T current properties that may be disregarded in classical biophysical studies drastically condition physiologically evoked burst firing and that these effects show a high degree of synaptic input specificity.

Methods

Ethical approval

Ethical approval was obtained for all experimental protocols from the Departmental Direction of Veterinary Services, Paris. All procedures involving experimental animals were carried out in accordance with the EU Council Directive 86-609. Every effort was made to minimize animal suffering and the number of animals used. For removal of tissues, animals were deeply anaesthetized with inhaled isoflurane and rapidly killed with a guillotine.

Preparation of brain slices and recordings

Brains were excised from 14- to 20-day-old Wistar rats or 30- to 45-day-old C57Blc6 wild-type or $Ca_V3.1^{-/-}$ mice (Kim *et al.* 2001). A block of tissue containing the thalamus was removed and placed in either an artificial cerebrospinal fluid (aCSF) or a sucrose based solution which was oxygenated (95% O_2–5% CO_2) and maintained at a temperature below 4°C. The two solutions had the following composition (in mM). aCSF: 125 NaCl, 2.5 KCl, 0.4 $CaCl_2$, 1 $MgCl_2$, 1.25 NaH_2PO_4, 26 $NaHCO_3$, 25 glucose, and 1 kynurenic acid; sucrose based solution: 230 sucrose, 2.5 KCl, 0.4 $CaCl_2$, 2 $MgCl_2$, 1.25 NaH_2PO_4, 26 $NaHCO_3$, 10 glucose, and 1 kynurenic acid, both solutions had a pH of 7.3 and an osmolarity of 310 mosmol l^{-1}. The block of tissue was glued, ventral surface uppermost, to the stage of a vibroslice (Leica VT1200S), and 220–280 μm thick horizontal slices containing the ventrobasal nucleus (VB) and the nucleus reticularis thalami (NRT) were prepared using the internal capsule and the medial lemniscus as landmarks. Slices were stored at room temperature in an oxygenated incubation chamber containing aCSF of the above composition, but without kynurenic acid and with 2 mM $CaCl_2$ for at least 1 h before being transferred to the recording chamber where they were continuously perfused (2.5 ml min^{-1}) with oxygenated recording solution of the same composition. Experiments were conducted at 32°C.

Using the patch-clamp technique (Optopatch amplifier, Cairn Research, Faversham, UK; Clampex 10, Molecular Devices, Sunnyvale, CA, USA), whole-cell recordings were performed in VB or NRT neurons visualized under Nomarski optics (Olympus BX51WI, ×60 lens). Electrodes were filled with the following solution (in mM): 140 potassium methanesulfonate, 0.1 $CaCl_2$, 5 $MgCl_2$, 1 EGTA, 10 Hepes, and 4 Na-ATP, 15 phosphocreatine and 50 units ml^{-1} creatine phosphokinase (pH 7.3, osmolarity 290 mosmol l^{-1}). Access resistance was monitored by measuring responses to small hyperpolarizing current pulses from resting membrane potential, and only data obtained from pipettes with access resistances of 8–13 MΩ with less than 20% change during the experiment were included in this study. Recordings were filtered by a 4-pole Bessel filter set at a corner frequency of 2 kHz and digitalized at 20 kHz.

To quantitatively compare LTS evoked with different T channel features, neurons were first submitted to prepulses delivered in voltage-clamp mode before instantaneously switching to the current-clamp mode. Neurons were

voltage clamped at a holding potential of −60 mV in-between protocols that were applied every 20 s.

Synaptic responses were induced using a glass pipette (6–8 μm tip diameter) filled with the extracellular medium. This stimulating electrode was positioned 25–60 μm from the recorded neuron to evoke IPSPs, in the medial lemniscus to evoke sensory EPSPs or in the internal capsule to evoke cortical EPSPs. The stimulus consisted of a 20–200 μs pulse of 10–40 V amplitude. Isolation of GABA IPSPs and glutamatergic EPSPs was achieved by the addition of 50 μM DL-2-amino-5-phosphonopentanoic acid (DL-APV) plus 10 μM 6-cyano-7-nitroquinoxaline-2,3-dione disodium (CNQX) and 1 μM SR95531 (6-imino-3-(4-methoxyphenyl)-1(6*H*)-pyridazinebutanoic acid hydrobromide; gabazine), respectively, to the perfusion medium.

Drugs and data analysis

TTA-P2 (3,5-dichloro-*N*-[1-(2,2-dimethyl-tetrahydro-pyran-4-ylmethyl)-4-fluoro-piperidin-4-ylmethyl]-benzamide) (compound (S)-5 in Fig. 3 of Shipe *et al.* 2008, Merck) was made up as 10 mM stock solution in dimethyl sulphoxide, kept at −20°C until use.

TTX was obtained from Latoxan (Valence, France), CNQX disodium salt, DL-APV, ZD7288, iberiotoxin and apamin from Tocris, and SR95531 from Sigma-Aldrich.

Recordings were analysed off-line using Igor 6 (WaveMetrics, Lake Oswego, OR, USA). Quantitative data in the text and figures are given as means ± SEM. Statistical significance was verified using Student's paired *t* test.

Dynamic-clamp and models

The T conductances were simulated using a real time version of the neuron environment (RT-NEURON developed by G. Le Masson, Wolfart *et al.* 2005) running under the Windows XP operating system. To inject the simulated T currents and monitor the membrane potential in real time, data transfer between the computer and the patch clamp amplifier was achieved by a PCI DSP Board (Innovative Integration). In order to achieve the computational speed required by the dynamic clamp technique, the Hodgkin–Huxley formalism was used to model thalamic T currents.

Thalamocortical T currents were simulated by the Hodgkin–Huxley-like model fitted to experimental data using empirical functions of voltage that was introduced by Huguenard & McCormick (1992) and further developed by Destexhe *et al.* (1998):

$$I_T = G_{Ca} m^2 h (V - V_{Ca}).$$

where G_{Ca} is the maximal conductance, V is the membrane potential of the neuron, $V_{Ca} = 180$ mV is the reversal potential for Ca^{2+} flux.

The activation (m) and inactivation (h) variables have voltage dependences defined as follows:

$$dm/dt = (m - m_\infty(V))/\tau_m(V)$$

$$dh/dt = (h - h_\infty(V))/\tau_h(V))$$

where

$$m_\infty(V) = 1/\{1 + \exp[-(V + 57)/6.2]\}$$

$$h_\infty(V) = 1/\{1 + \exp[(V + 81)/4]\}$$

$$\tau_m(V) = \{0.612 + 1/\{\exp[-(V + 132)/16.7] + \exp[(V + 16.8)/18.2]\}\}/Q$$

$$\tau_h(V) = \{28 + \exp[-(V + 22)/10.5]\}/Q \quad \text{for} \quad V \geq -81\ \text{mV}$$

$$\tau_h(V) = \{\exp[(V + 467)/66.6]\}/Q \quad \text{for} \quad V < -81\ \text{mV}.$$

The variable Q was set to 2.5 corresponding to an experimental temperature of 34°C assuming a Q_{10} value of 2.5 with an extracellular Ca^{2+} concentration of 2 mM (Coulter *et al.* 1989).

Based on Destexhe *et al.* (1996), a similar model was used to simulate T current in NRT neurons with voltage dependences of the m and h variable defined by:

$$m_\infty(V) = 1/\{1 + \exp[-(V + 50)/7.4]\}$$

$$h_\infty(V) = 1/\{1 + \exp[(V + 78)/5]\}$$

$$\tau_m(V) = \{3 + 1/\{\exp[-(V + 100)/15] + \exp[(V + 25)/10]\}\}/Q$$

$$\tau_h(V) = \{85 + 1/\{\exp[-(V + 405)/50] + \exp[(V + 46)/4]\}\}/Q.$$

Results

Ca^{2+} activated conductances are not required for high-frequency firing in TC neurons

The activation of T channels induces both a transient depolarization and Ca^{2+} entry that may, in turn, lead to activation of other ion channels. Among them, Ca^{2+}-dependent small and big K^+ channel conductances associated with SK and BK channels, respectively, have

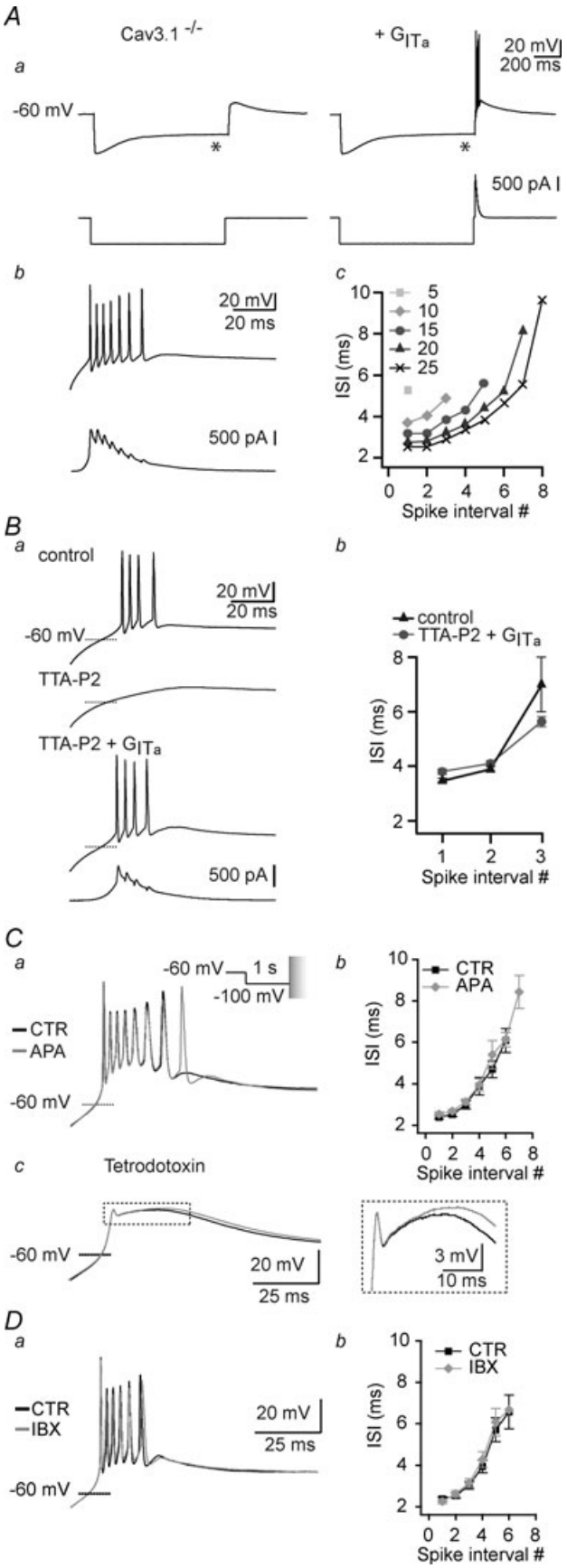

been reported in thalamic sensory nuclei (Sailer *et al.* 2004; Sausbier *et al.* 2006), along with a Ca^{2+}-activated non-selective cationic current (Williams *et al.* 1997). However, it is still unknown whether recruitment of these conductances by the T current-mediated Ca^{2+} entry is required to shape the LTS and its associated high-frequency firing. To answer this question we injected artificial T current (IT_a), which mimicked the T channel mediated charge influx in the absence of the associated Ca^{2+} entry in ventrobasal (VB) TC neurons from Cav3.1$^{-/-}$ mice, which lack endogenous T channels. In these neurons, no rebound LTS could be evoked at the end of a hyperpolarizing current step, as expected from the absence of endogenous T current, and only a small transient depolarization due to I_h tail current was observed (Fig. 1*Aa* left). However, injection of IT_a fully restored the LTS generation and its associated

Figure 1. The high-frequency firing elicited by an LTS is reproduced by artificial T current (IT_a) and does not require SK and BK channel activation
Aa, as illustrated in the left traces recorded in current clamp mode, a hyperpolarizing current step (bottom trace) does not evoke a rebound LTS in a Cav3.1$^{-/-}$ mouse TC neuron (top trace). The small depolarization observed at the end of the hyperpolarizing current step reflects the activation of the h-current that appears as a depolarizing sag (*) in the hyperpolarizing response to the intracellular current step. In the same TC neuron, the LTS is restored by injection of an artificial T conductance (G_{ITa}) using the dynamic-clamp technique. *b*, enlarged records of the LTS and associated action potentials. Note that somatic injection of an artificial T conductance is sufficient to induce a burst of action potentials that mimics the activity recorded in control mice. Bottom trace presents the injected current generated by the artificial T conductance during the burst. *c*, ISIs are plotted against spike interval position for increasing values of G_{ITa} in nS. *Ba*, native rebound LTS was evoked in a TC neuron from a wild-type mouse at the offset of a 1 s hyperpolarization to −100 mV in control condition (top trace). Application of 3 μM TTA-P2 fully blocked the LTS (middle trace), which was then restored by injection of G_{ITa} (10 nS, bottom trace). *b* graph illustrating for this neuron the ISI as a function of the spike interval position for native and G_{ITa}-induced LTS (number of trials = 5). Note the similarity in the dynamics of native and artificial LTS bursts. *C*, superimposed traces in *a* depict LTSs evoked in a TC neuron from a wild-type mouse at the offset of a 1 s hyperpolarization to −100 mV in control condition and in the presence of apamin (300 nM). To accurately control the T-channel state, the hyperpolarization required to de-inactivate the T channel population was performed in voltage-clamp mode before switching to current-clamp mode to allow the membrane to repolarize and generate a rebound LTS. Note that block of the SK channels prolonged the burst by one action potential but had no effect on the firing frequency. The graph in *b* illustrates the ISI as a function of the spike interval position in control condition and in the presence of apamin ($n = 7$). *c*, in the presence of TTX (1 μM), application of apamin reveals a small prolongation of the LTS. Enlargements of the traces are presented in the inset. *D*, same protocols as in *C* to test the effect of iberotoxin (100 nM). Note that block of the BK channels has no effect on the number of action potentials within the burst ($n = 7$).

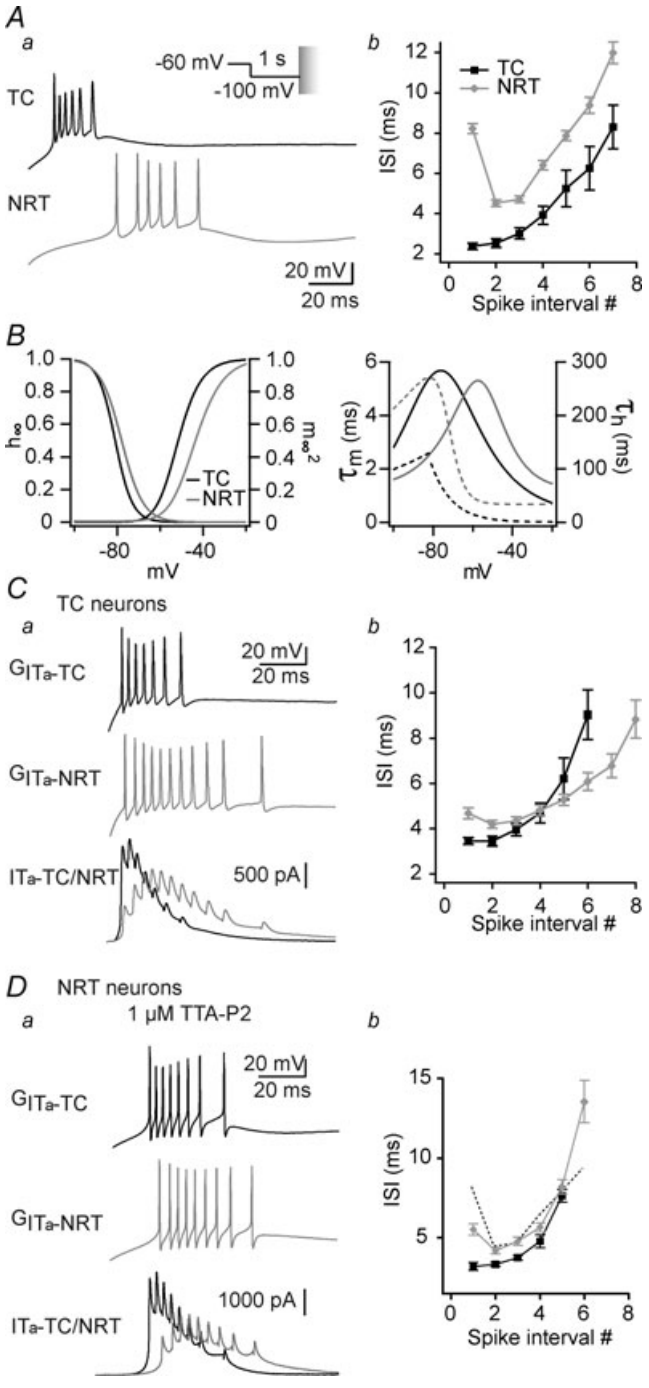

Figure 2. The temporal signature of the burst closely depends on the biophysical properties of IT
Aa, typical traces illustrating the difference in burst firing pattern evoked at the offset of a 1 s hyperpolarization to −100 mV in TC (black trace) and NRT (grey trace) neurons. The conditioning hyperpolarizing pre-pulse was performed in voltage-clamp mode before switching to current-clamp mode to allow the membrane to repolarize and generate a rebound LTS. *b*, graph showing the mean duration of the ISI as a function of the spike interval position. Bursts in TC neurons are characterized by a continuous increase in ISI called the 'decelerando pattern' ($n = 12$), whereas bursts in NRT neurons display an initial decrease in ISI followed by a progressive increase, called the 'accelerando-decelerando pattern' ($n = 12$). *B*, biophysical parameters of T conductances modelled according to the T channel properties expressed in TC (black traces) and NRT (grey traces) neurons (see Methods for details of the model). Left graph: steady-state inactivation (h_∞) and activation (m^2_∞) voltage dependencies. Right graph: time constant of the activation (τ_m, continuous lines) and inactivation (τ_h, dotted lines) kinetics as a function of membrane potential. *C*, using the same protocol as in *A*, rebound bursts were evoked in a Cav3.1$^{-/-}$ TC neuron by introducing the artificial T conductance mimicking T channels expressed in either TC (G_{ITa-TC}, top black trace in *a*) or NRT neurons ($G_{ITa-NRT}$, middle grey trace in *a*). In both the typical traces in *a* and the graph of the mean ISIs (*b*, $n = 8$), note that injection of the NRT T conductance into the soma of a TC neuron results in a rebound burst displaying the typical 'accelerando-decelerando' pattern observed in NRT neurons. Note also in the superimposed injected current traces (bottom traces in *a*) that in both cases the shorter ISI in the burst occurred when IT_a is maximal. *D*, same protocol as in *C* performed in NRT neurons of wild-type mouse recorded in the presence of 1 μM TTA-P2 to block endogenous T channels. Injection of artificial TC (G_{ITa-TC}, black trace) or NRT ($G_{ITa-NRT}$, grey trace) T conductances results in rebound bursts of action potentials that reproduce the 'decelerando' and 'accelerando-decelerando' patterns, respectively (*b*, $n = 8$). Mean ISI of high-frequency bursts generated by native NRT T current (see *Ab*) are indicated by the dotted line for comparison.

high-frequency burst of action potentials (APs) upon membrane repolarization (Fig. 1*Aa* and *b*) in the absence of Ca^{2+} influx. In all recorded neurons, the number and frequency of APs within the burst was closely dependent on the amplitude of the artificial T conductance (Fig. 1*Ac*), with the largest burst and highest frequency obtained for the maximal conductance. The similarity between artificial and native rebound LTS was further assessed in the same neurons by comparing high-frequency bursts of APs generated by endogenous T current and those restored by injecting IT_a following the block of the native T-channels by TTA-P2 (Dreyfus *et al.* 2010; Fig. 1*B*). Comparison of inter-spike intervals (ISIs) shows that the temporal dynamics of APs within the native and artificial bursts are similar (Fig. 1*Bb* and see also Fig. 1*Ac*, *Cb* and *Db*). This result shows that the high-frequency firing pattern depends upon the biophysical properties of the T channels rather than the activation of Ca^{2+}-dependent currents. To further evaluate whether Ca^{2+}-dependent K^+ channel conductances significantly participate in LTS and its associated high-frequency firing, bursts were evoked in VB neurons from wild-type mice in the presence of the SK channel antagonist apamin or the BK channel antagonist iberotoxin. To ensure an accurate and reproducible control of the T channel states, prolonged hyperpolarization required to de-inactivate the T channel population was performed in voltage-clamp mode prior to switching to current-clamp mode, allowing the membrane to repolarize and generate a rebound LTS. Block of SK channels by apamin induced a slight lengthening by

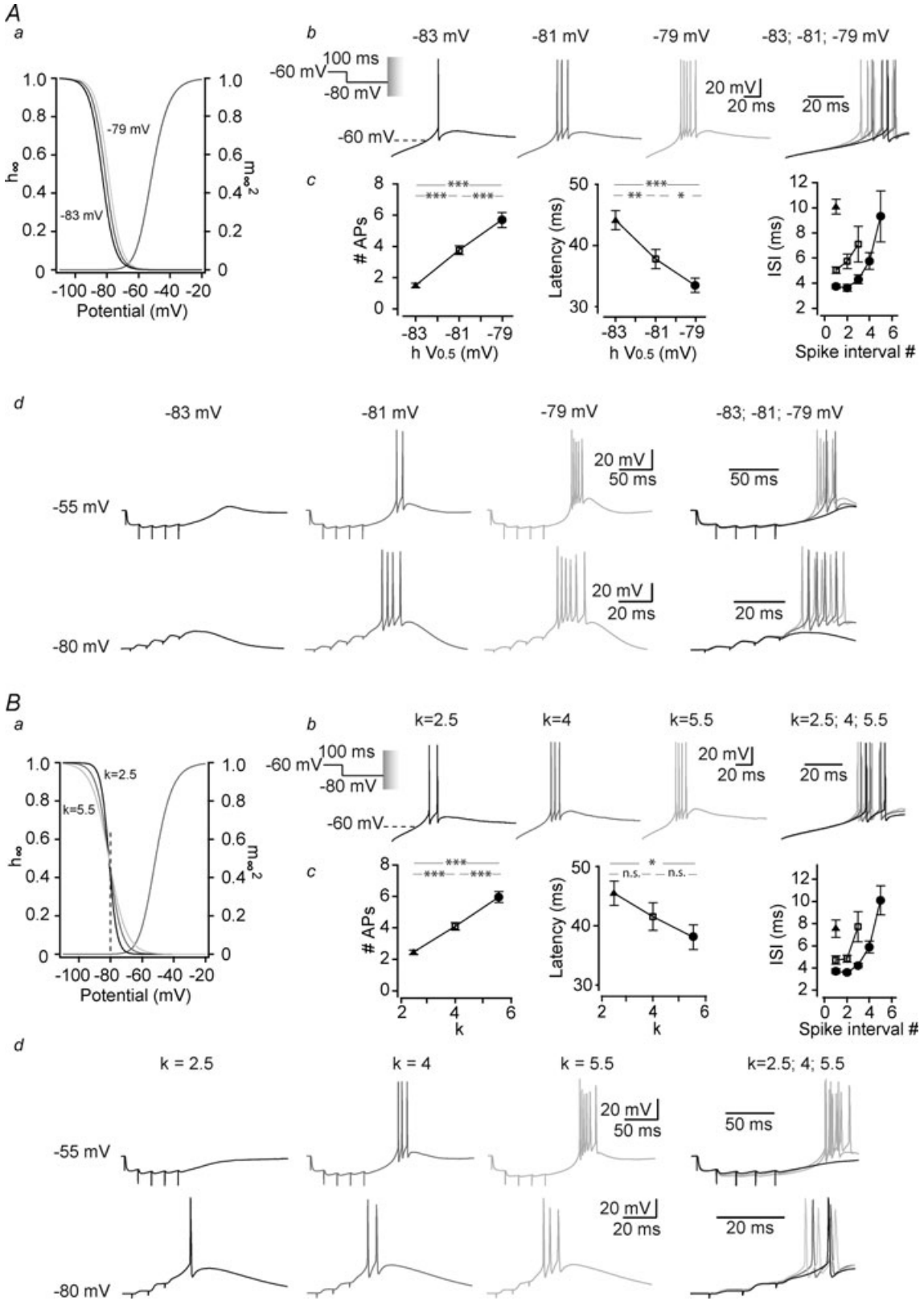

Figure 3. Small modifications in steady-state inactivation voltage dependence of the T channels drastically modify the bursting pattern of TC neurons evoked by physiological protocols
A, responses of a Cav3.1$^{-/-}$ TC neuron to a 100 ms hyperpolarization to −80 mV were successively recorded while injecting artificial T conductances displaying normal ($V_{0.5}$ = −81 mV), slightly hyperpolarized ($V_{0.5}$ = −83 mV)

one action potential of the burst in 5 out of the 7 neurons (number of APs: control: 6.7 ± 0.4, apamin: 7.5 ± 0.3, $P \leq 0.01$, $n = 7$, Fig. 1*Ca*). However, neither the frequency of firing within the burst (Fig. 1*Cb*) nor the latency of the first AP in the burst were modified (time from end of step to first AP: control: 18.4 ± 1.7 ms, apamin: 19.5 ± 1.6 ms, $P = 0.1$, $n = 7$). As shown in Fig. 1*Cc*, similar experiments performed in the presence of TTX revealed that block of SK channels induced a very small increase in the LTS duration (half-width of the LTS: control: 47.5 ± 2.8 ms, apamin: 50.2 ± 2.8 ms, $P \leq 0.01$, $n = 6$) and amplitude (maximal membrane potential reached by the LTS waveform: control: -38.6 ± 1.5 mV, apamin: -37.5 ± 1.4 mV, $P \leq 0.005$, $n = 6$). This suggests that SK channel activation modestly limits burst firing by accelerating the LTS repolarizing phase. Similar experiments were thereafter conducted in the presence of iberotoxin. Block of the BK K^+ channels had no effect either on the number of APs in the burst (number of APs: control: 6.2 ± 0.2, iberotoxin: 6.2 ± 0.2, Fig. 1*Da*) or on the frequency of firing (Fig. 1*Db*) in seven TC neurons. Thus, activation of Ca^{2+}-activated K^+ channels by Ca^{2+} entry associated with LTS has little effect on the burst firing pattern.

High-frequency bursts dynamics

A fundamental issue in information processing is how presynaptic trains of APs shape the response dynamics of the postsynaptic neuron which are often highly non-linear. Both the rate of firing and the temporal distribution of APs of the presynaptic neuron are critical to drive the postsynaptic targets (Lisman, 1997; Swadlow *et al.* 2005). As shown in Fig. 2*Aa*, while both the TC neurons and the GABAergic neurons of the NRT are able to discharge high-frequency bursts of APs through activation of T currents, the bursts in each of these two neuronal types present a specific temporal signature (Domich *et al.* 1986). Bursts in TC neurons are characterized by a continuous decrease in firing frequency that generates a signature called the 'decelerando' pattern whereas the burst signature in NRT neurons is characterized by an initial increase followed by a progressive decrease in firing frequency called the 'accelerando-decelerando' pattern (Fig. 2*Ab*). We then investigated whether such differences in burst signature may reflect differences in the biophysical properties of the T currents expressed in TC and NRT neurons. Indeed, the Cav3.1 T channel isotype, specifically expressed in TC neurons, generates a fast transient current whereas both the Cav3.2 and 3.3 isotypes that are expressed in NRT neurons generate a relatively slower activating and inactivating current (Huguenard & Prince, 1992). Therefore, to evaluate the role of these T channel biophysical properties in the generation of the specific burst signature, IT_a designed with TC and NRT current properties, respectively (Fig. 2*B* and see Methods) were successively injected into TC neurons from Cav3.1$^{-/-}$ mice.

As already shown in Fig. 1, injection of TC IT_a restored rebound LTS generation with its associated firing being similar in both frequency and 'decelerando' pattern to that observed in TC neurons from wild-type mice (Fig. 2*C*). On the other hand, when NRT IT_a was injected into the same TC neurons the restored burst firing displayed a clear 'accelerando-decelerando' pattern that was qualitatively similar, though less intense, to the NRT burst signature (Fig. 2*C*). Analysis of the injected IT_a during LTS in both cases showed that the higher firing frequency within the burst is reached when the amplitude of the current is maximal (Fig. 2*Ca*). Because of its fast gating kinetics, TC IT_a is already maximal when the first AP of the burst is evoked and decreases thereafter (Fig. 2*Ca*, black line). As a consequence the firing frequency continuously decelerates within the burst. Conversely, because of

or depolarized ($V_{0.5} = -79$ mV) inactivation voltage dependence (see graph of the *I–V* curves in *a*). The conditioning hyperpolarizing pre-pulse was performed in voltage-clamp mode before switching to current-clamp mode to allow the membrane to repolarize and generate a rebound LTS. As illustrated by the typical traces in *b* and quantified in *c* ($n = 9$), slight hyperpolarization of the T current inactivation decreases the number of spikes within a burst, increases the latency of firing (delay between repolarization onset and the first action potential) and the ISI. The reverse was observed with slight depolarization of the steady-state inactivation. *d*, similar experiments were performed in current clamp mode using either a train of GABAergic IPSPs (5 stimuli at 50 Hz of the NRT input) from a holding potential of -55 mV to evoke a rebound LTS (top records) or a train of corticothalamic EPSPs (4 stimuli at 100 Hz, bottom records) to trigger an LTS (bottom records) from a holding potential of -80 mV. Typical records illustrate that small modifications in inactivation voltage dependence strongly affect the ability of synaptically evoked T current to induce an LTS large enough to trigger a burst of action potentials. *B*, same protocols as in *A* were performed in Cav3.1$^{-/-}$ TC neuron while slightly modifying the voltage sensitivity of the steady-state inactivation by adjusting the slope factor of the inactivation curve around the control *k* value of 4 without modifying the $V_{0.5}$ (see graph in *a*). Maximal excitability is obtained while injecting IT_a with the shallower slope ($k = 5.5$; *b* and *c*, $n = 7$) that allowed a larger recovery from inactivation during the 100 ms long hyperpolarization to -80 mV (see dotted line in *a*). As illustrated in *d*, similar results are observed when LTSs were evoked by the NRT input and corticothalamic feedback (Student's paired *t* test: n.s., not significant; $^*P < 0.5$; $^{**}P < 0.01$; $^{***}P < 0.005$).

the slow kinetics of the NRT IT_a, current amplitude still increases after the first AP (Fig. 2*Ca*, grey line), thus inducing an initial phase of acceleration in firing frequency. To further check that T current kinetics are fundamental in defining the burst signatures, similar experiments were performed in NRT neurons of wild-type mice in which endogenous T currents were suppressed by continuous perfusion of the specific T channel antagonist TTA-P2 (1 μM, Supplemental Fig. 1*A*; Dreyfus *et al.* 2010). In these conditions, injection of NRT but not TC IT_a in the soma of NRT neurons generated burst firing that displayed the expected typical 'accelerando-decelerando' pattern (Fig. 2*D*). However, this artificially generated signature was reduced in comparison to that observed with endogenous T current (Fig. 2*D*). Such a difference may be due to the somatic localization of the IT_a injection since modelling studies have proposed that the temporal signature of the NRT neurons arises in part from the dendritic localization of endogenous T channels (Destexhe *et al.* 1996). The lack of Ca^{2+} entry when injecting dynamic-clamp currents may also be a limiting parameter to fully mimic the native LTS dynamic in NRT neurons since SK channels have been shown to closely control burst firing in these neurons (Avanzini *et al.* 1989; Bal & McCormick, 1993). Indeed, although the 'accelerando-decelerando' pattern of the burst generated by endogenous T current is still present upon apamin application in NRT neurons (Supplemental Fig. 1*B*), we observed an attenuation of this signature (1st ISI: control: 13.1 ± 2.9 ms; apamin: 7.5 ± 1.5 ms; $P \leq 0.01$, $n = 6$) conjointly to a drastic prolongation of the burst (number of AP: control 6.0 ± 0.7; apamin: 53.9 ± 7.7 $P \leq 0.001$, $n = 6$). In conclusion, the presence of the LTS firing signature in NRT neurons somatically injected with artificial NRT IT_a and its loss when artificial TC IT_a was used clearly suggest that the specific kinetics of the T currents in the NRT impact the burst pattern.

Small changes in T current biophysical properties strongly affect the high-frequency burst firing of synaptically generated LTSs

The limited precision of the electrophysiological characterization of native T currents *in situ* (see for example Fig. 1 in Huguenard & McCormick, 1992), the regulation of their properties by endogenous modulators (Lambert *et al.* 2006), and the expression of a variety of splice variants (Perez-Reyes, 2003) are some of the possible reasons that might explain the different biophysical parameter values reported for a given T channel isoform. Since our previous experiments predicted that such diversities may drastically modify the burst generation, we next evaluated their impact on the thalamic excitability by systematically introducing in the model of IT_a small variations in the voltage dependent-gating of the T channel. Because burst generation and firing patterns were totally restored by IT_a injection in TC neurons of $Cav3.1^{-/-}$ mice but not in NRT neurons, we thereafter focused our study on the LTS-mediated high-frequency burst firing in TC neurons.

Shifting the voltage dependence of the steady-state inactivation by 2 mV toward more hyperpolarized or depolarized potentials (Fig. 3*Aa*) had no impact on the burst generation and its associated firing when rebound LTSs were evoked at the end of a non-physiological 1 s long hyperpolarization to -100 mV that allowed complete de-inactivation of the artificial T channels in every condition (Supplemental Fig. 2). However, when hyperpolarization that mimicked physiological activities was used, such small modifications in the voltage dependence of inactivation affected the number of T channels recovering from inactivation and hence had a drastic effect on the burst generation. As shown in Fig. 3*Ab* and *c*, when IT_a displaying a hyperpolarized steady-state inactivation curve was injected into $Cav3.1^{-/-}$ TC neurons, rebound burst evoked at the end of 100 ms long hyperpolarizing steps to -80 mV presented a greatly reduced number of APs, longer latency and slower intra-burst frequency compared to control condition (i.e. $V_{0.5} = -81$ mV). Conversely, 2 mV depolarization of the inactivation voltage dependence induced a clear increase in the burst firing in both the number and the frequency of APs, and shortened its latency.

The impact on the TC excitability of small changes in the inactivation gating following physiological hyperpolarization was confirmed and enlarged by experiments where the LTS was elicited by synaptic stimulations and not by direct somatic current injection. In TC neurons, short hyperpolarizations are typically induced by the brief bursts of GABAergic postsynaptic potentials originating from the NRT. Therefore, local electrical stimulations of the afferent NRT fibres were performed to elicit composite GABA-A/B inhibitory postsynaptic potentials (IPSPs) while injecting IT_a. As shown in Fig. 3*Ad* and quantified in Table 1, the rebound bursts that were readily evoked at the end of the train of IPSPs displayed a similar sensitivity toward changes in voltage dependence of the steady-state inactivation as the LTS evoked by a hyperpolarizing current pulse. Similar results were obtained for LTS triggered by the corticothalamic glutamatergic excitatory postsynaptic potentials (EPSPs) that were elicited by minimal stimulation of the internal capsule while maintaining the TC neurons at -80 mV (Fig. 3*Ad*, Table 1). These data suggest that, because recovery from inactivation of the T channels occurs near the voltage of half steady-state inactivation under physiological conditions, small modifications of the inactivation voltage dependence will have a profound effect on TC neuron excitability and synaptic integration.

Table 1. LTS burst firing evoked by synaptic inputs

Inactivation $V_{0.5}$	IPSPs ($n = 6$)				Corticothalamic EPSPs ($n = 6$)				Lemniscal EPSPs ($n = 6$)			
	−83 mV	−81 mV	−79 mV	−83/81; −81/79; −83/79	−83 mV	−81 mV	−79 mV	−83/81; −81/79; −83/79				
Number of APs	0.0 ± 0.0	2.6 ± 0.8	5.3 ± 0.6	*; **; ***	0.5 ± 0.2	2.4 ± 0.3	4.5 ± 0.6	***; *; ***				
Latency (ms)	—	138.0 ± 6.7	126.3 ± 5.7	–; **; –	43.9 ± 1.6 ($n = 3$)	41.1 ± 2.0	36.8 ± 1.1	–; *; –				
1st ISI (ms)	—	8.5 ± 1.5	3.8 ± 0.5	–; *; –	—	6.5 ± 0.8	4.4 ± 0.8	–; *; –				
Inactivation slope (k)	IPSPs ($n = 6$)				Corticothalamic EPSPs ($n = 6$)				Lemniscal EPSPs ($n = 6$)			
	2.5	4	5.5	2.5/4; 4/5.5; 2.5/5.5	2.5	4	5.5	2.5/4; 4/5.5; 2.5/5.5				
Number of APs	0.0 ± 0.0	3.5 ± 0.4	6.0 ± 0.4	***; *; ***	1.0 ± 0.3	2.2 ± 0.2	3.5 ± 0.3	***; ***; ***				
Latency (ms)	—	135.1 ± 4.4	147.5 ± 15.2	–; n.s.; –	33.6 ± 1.9 ($n = 3$)	31.1 ± 2.7	28.9 ± 2.0	**; n.s.; ***				
1st ISI (ms)	—	5.5 ± 0.9	3.4 ± 0.4	–; *; –	—	7.0 ± 0.9	5.3 ± 0.8	–; *; –				
Activation $V_{0.5}$	IPSPs ($n = 6$)				Corticothalamic EPSPs ($n = 6$)				Lemniscal EPSPs ($n = 6$)			
	−59 mV	−57 mV	−55 mV	−59/57; −57/55; −59/55	−59 mV	−57 mV	−55 mV	−59/57; −57/55; −59/55				
Number of APs	3.3 ± 0.5	2.1 ± 0.3	0.5 ± 0.3	***; **; ***	3.9 ± 0.7	2.4 ± 0.2	0.6 ± 0.3	***; ***; ***				
Latency (ms)	122.0 ± 4.3	137.5 ± 6.5	144.0 ± 3.0 (n = 2)	**; –; –	34.0 ± 1.1	41.8 ± 2.0	44.5 ± 1.5 (n = 3)	**;–; –				
1st ISI (ms)	4.1 ± 0.5	4.9 ± 0.7	—	n.s.; –; –	5.3 ± 1.0	5.9 ± 0.9	—	n.s.; –; –				
Activation slope (k)	IPSPs ($n = 6$)				Corticothalamic EPSPs ($n = 6$)				Lemniscal EPSPs ($n = 6$)			
	4	6	8	4/6; 6/8; 4/8	4	6	8	4/6; 6/8; 4/8	4	6	8	4/6; 6/8; 4/8
Number of APs	0.5 ± 0.3	2.5 ± 0.3	0.5 ± 0.3	*; *; n.s.	1.1 ± 0.5	2.1 ± 0.3	3.1 ± 0.4	*; n.s; *	3.7 ± 0.2	2.3 ± 0.2	1.6 ± 0.3	**; **; **
Latency (ms)	154.4 ± 21.3 ($n = 2$)	136.8 ± 7.7	116.3 ± 3.7 ($n = 2$)	–; –; –	42.1 ± 2.2 (n = 3)	39.9 ± 2.2	35.6 ± 1.6	*; *; *	9.1 ± 1.6	11.0 ± 1.7	13.1 ± 2.8	n.s.; n.s.; n.s.
1st ISI (ms)	—	7.2 ± 1.0	—	–; –; –	—	6.2 ± 0.7	5.2 ± 0.7	–; n.s.; –	5.3 ± 0.6	6.1 ± 1.0	5.2 ± 0.6	n.s.; n.s.; n.s.

Student's paired t test: n.s., not significant; $^{*}P < 0.5$; $^{**}P < 0.01$; $^{***}P < 0.005$.

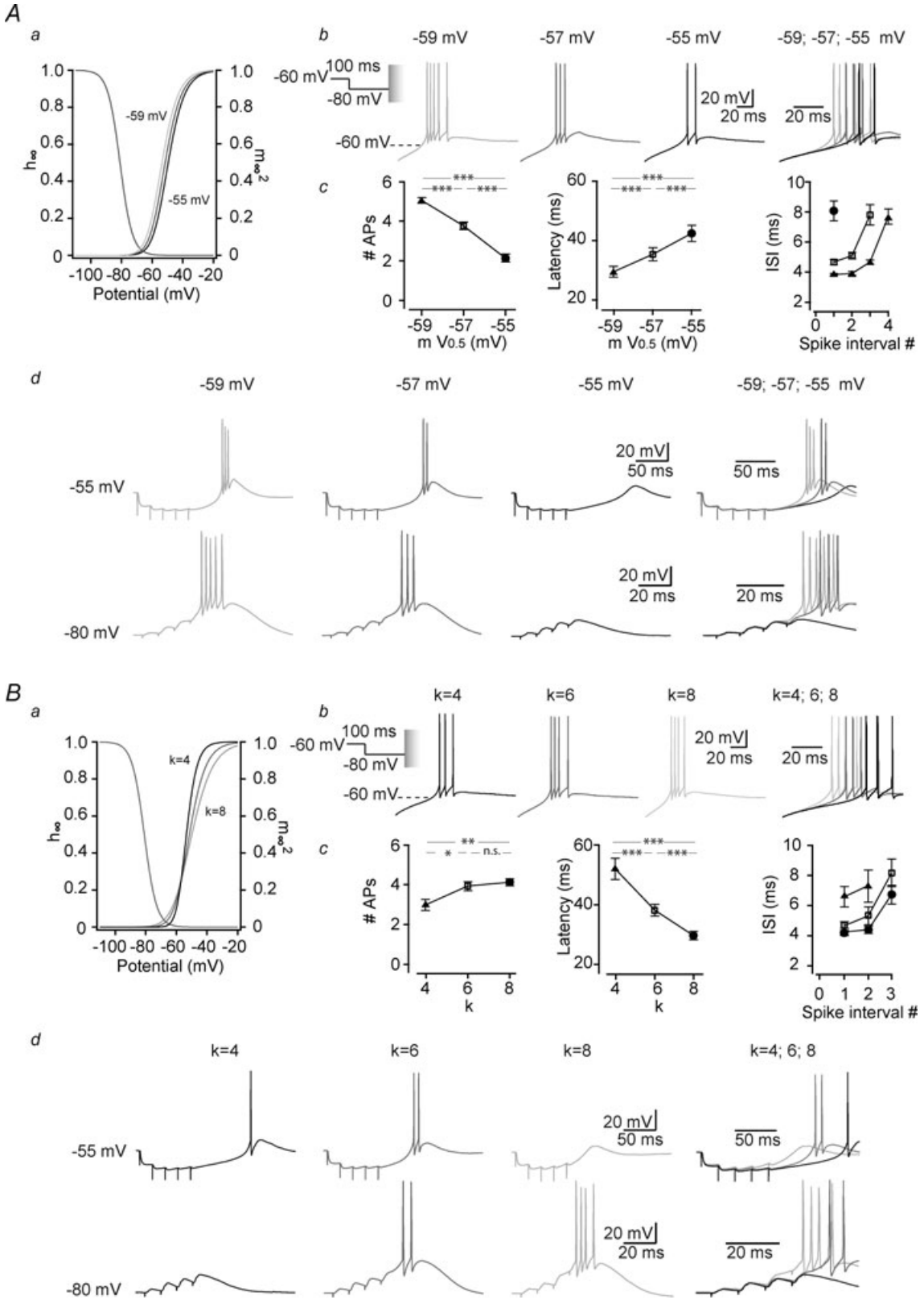

Figure 4. Small modifications in activation voltage dependencies of the T channels drastically modify the bursting pattern of TC neurons

A, same protocols as in Fig. 3 were performed in Cav3.1$^{-/-}$ TC neuron while injecting IT_a with normal ($V_{0.5} = -57$ mV), slightly hyperpolarized ($V_{0.5} = -59$ mV) or depolarized ($V_{0.5} = -55$ mV) activation voltage

This conclusion is reinforced by the results obtained when injecting IT_a for which the slope of the inactivation *I–V* curve was slightly modified without varying the voltage of half-inactivation. Indeed, as shown in Fig. 3*B*, although steady-state inactivation occurring around −80 mV is hardly modified by such changes in the inactivation slope (see dotted line in Fig. 3*Ba*, $h_{\infty-80\text{mV}} = 0.40$, 0.44 and 0.45 for slope factor $k = 2.5$, 4 and 5.5, respectively), these minimal changes are still able to alter the LTS mediated high-frequency firing (Fig. 3*Bc*, Table 1).

We then investigated whether small modifications in activation voltage dependence can similarly affect bursts generated by either short voltage-clamped prepulses to −80 mV, trains of IPSPs or corticothalamic EPSPs. The results summarized in Fig. 4*A* clearly show that 2 mV shifts of the half-activation voltage in the hyperpolarizing or depolarizing direction of the activation *I–V* curve induced a drastic increase or decrease of the LTS associated firing, respectively. In every condition, the most hyperpolarized activation voltage dependence facilitates burst generation resulting in a higher number of APs, a shorter latency and a higher intraburst frequency (Fig. 4*Ac*, Table 1).

Modification of gating properties at resting membrane potential constrains neuron integrative properties according to the synaptic events

Surprisingly, slightly modifying the slope of the activation *I–V* curve without changing the voltage of half activation led to contrasting results according to the nature of the event that triggered burst generation. Thus, the smallest and slowest bursts generated by 100 ms hyperpolarization to −80 mV (Fig. 4*Bb*) were obtained when IT_a incorporated a steeper slope. Similar results were found with LTS triggered by corticothalamic inputs (Fig. 4*Bd*, Table 1). Since this modification facilitates activation of the artificial T channels in the voltage range between −57 mV and −20 mV (Fig. 4*Ba*), these data appear at first glance in contradiction with the results obtained in the condition of a hyperpolarized value for the half-activation voltage ($V_{0.5} = -59$ mV) (Fig. 4*A*). Moreover, when rebound bursts were evoked by GABAergic IPSPs, both steeper and shallower slopes of activation reduced the burst firing (Fig. 4*Bd*, Table 1).

In order to understand the mechanism responsible for such discrepancy, rebound LTSs were generated by short hyperpolarization to −80 mV using IT_a designed with marked slope differences while closely monitoring the injected dynamic-clamp current as well as the inactivation and activation states of the model. As shown in Fig. 5*Aa*, although a steep slope facilitates channel activation for voltages higher than −57 mV, it actually reduces channel activation at more hyperpolarized potentials. As a consequence, T channels are recruited late during the initial phase of repolarization from −80 mV, delaying this repolarization (latency: $k = 2$: 69.9 ± 7.6 ms; compared to control $k = 6$: 38.1 ± 2.0 ms, $P \leq 0.001$, $n = 8$). Therefore, significant T channel inactivation occurred during such slow repolarization and a small number of channels were available when the membrane potential reached the LTS threshold (percentage of inactivated channels: $k = 2$: 92.9 ± 1.1; compared to control $k = 6$: 82.3 ± 0.9 at the time of the first AP, $P \leq 0.001$, $n = 8$). A small IT_a was evoked and the burst was minimal (number of AP: $k = 2$: 1.0 ± 0.3; compared to control $k = 6$: 3.9 ± 0.2, $P \leq 0.001$, $n = 8$; Fig. 5*Ab*). Conversely, a shallower slope allowed channel activation at potentials close to −80 mV, accelerating membrane repolarization (latency: $k = 10$: 23.9 ± 1.2 ms compared to control $k = 6$: 38.1 ± 2.0 ms, $P \leq 0.001$, $n = 8$) and minimizing T channel inactivation before LTS generation (percentage of inactivated channels: $k = 10$: 78.0 ± 1.0 compared to control $k = 6$: 82.3 ± 0.9, $P \leq 0.001$, $n = 8$; Fig. 5*Ab*). We then hypothesized that the effect of the slope of IT_a on the LTS generation should be different when the recruitment of T-channels at hyperpolarized potentials does not contribute to the repolarization kinetics. Indeed, when rebound LTSs were evoked after 1 s long hyperpolarization to −100 mV, activation of the h-current (I_h, see the depolarizing sag of the hyperpolarizing response to the intracellular current step in Fig. 1*Ca*) greatly accelerated the membrane repolarization, and the participation

dependence (see graph of the *I–V* curves in *a*). As illustrated in the typical traces in *b*, small modifications in the T conductance activation voltage dependence strongly affect the neuron high-frequency firing output. Hyperpolarizing the activation curve increases the number of spikes within the burst and reduces the latency and the ISI (c, $n = 8$). Traces in *d* show that these effects are also present when LTSs are triggered by synaptic events evoked as in Fig. 3*Ad*. *B*, the effects of slight modifications in the activation slope factor ($k = 4$, 6 and 8) were similarly investigated while triggering rebound LTS with 100 ms long hyperpolarization to −80 mV. As shown in *b* and quantified in *c*, although the steeper slope ($k = 4$) generated the more hyperpolarized activation gating of the artificial T conductance on a large range of potentials (see curves between −55 and −20 mV in *a*), it decreases the number of spikes per burst, and increases both latency of firing and ISI ($n = 8$). Similar results are obtained when LTSs are evoked by corticothalamic stimulations (bottom traces in *d*, $n = 6$). However, when rebound LTSs are triggered by stimulating GABAergic inputs, the maximal excitability is observed with the control slope factor of $k = 6$ but both steeper ($k = 4$) and shallower ($k = 8$) slopes induces a decrease in action potential firing (top traces in *d*, $n = 4$) (Student's paired *t* test: n.s., not significant; $^*P < 0.5$; $^{**}P < 0.01$; $^{***}P < 0.005$).

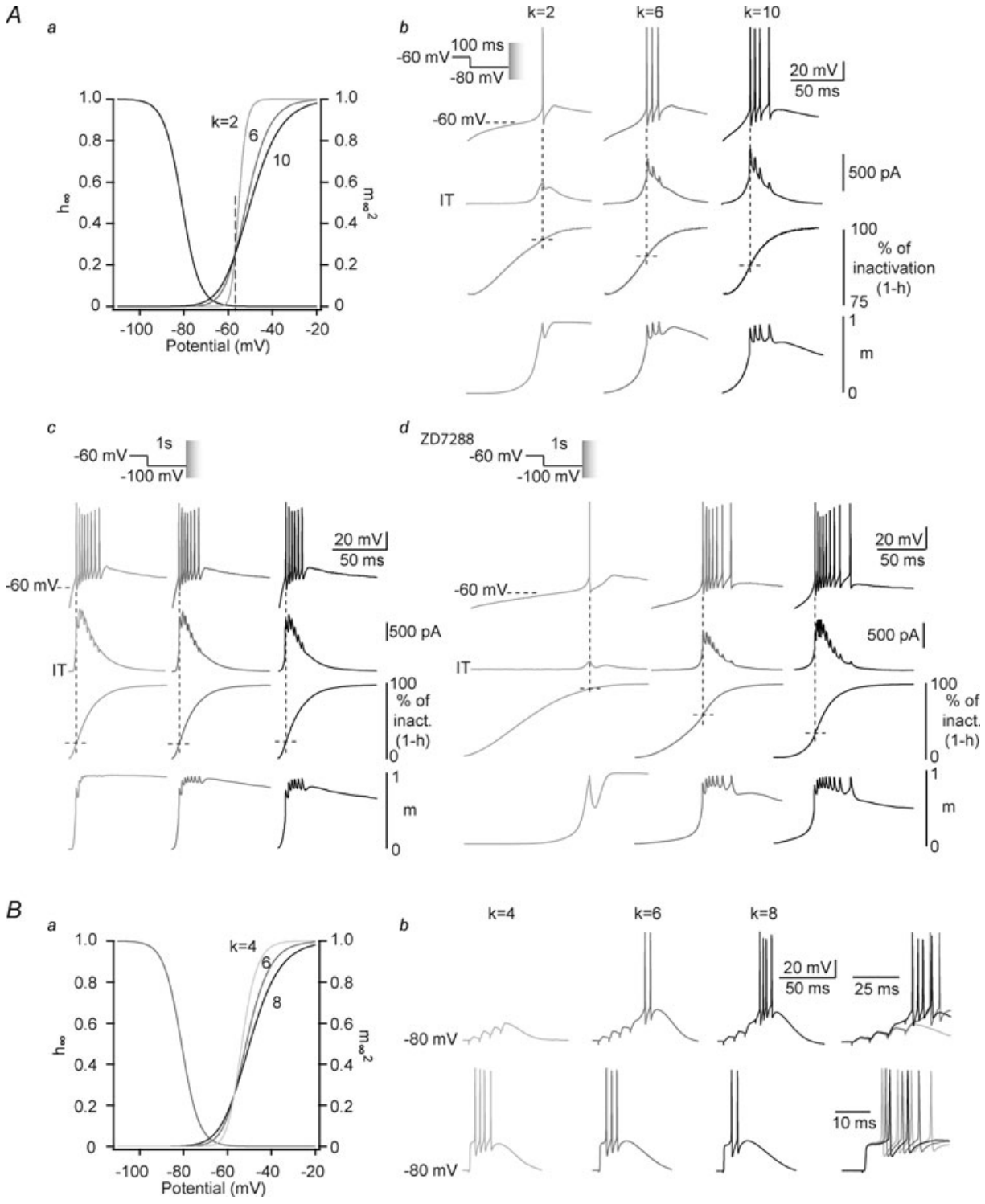

Figure 5. In TC neurons, bursting response to different synaptic inputs is specifically conditioned by the base of the activation curve

Aa, *I–V* curves of artificial T conductances with activation slope factor *k* equal to 2, 6 and 10. Note that the shallowest slope facilitates activation gating at membrane potential below −57 mV. Conversely, for potentials above −57 mV, T channel activation is enhanced with the steepest slope. *b*, LTSs (top traces) are evoked at the end of a 100 ms hyperpolarization to −80 mV in a TC neuron from Cav3.1$^{-/-}$ mice in the presence of IT_a (middle traces) with activation slope factor *k* equal to 2, 6 and 10. The conditioning hyperpolarizing pre-pulse was performed in voltage-clamp mode before switching to current-clamp mode to allow the membrane to repolarize

of the IT_a in this repolarization became negligible (latency: $k = 2$: 9.3 ± 0.5 ms, $k = 6$: 8.8 ± 0.5 ms, $k = 10$: 8.6 ± 0.5 ms, $P > 0.05$, $n = 7$). In this condition, the channel inactivation that occurred before the membrane potential had reached the LTS threshold was small and equivalent for each slope factor (percentage of inactivated channels: $k = 2$: 20.2 ± 1.2, $k = 6$: 19.1 ± 1.5, $k = 10$: 18.3 ± 1.3, $P > 0.05$, $n = 7$). Therefore, the effect of slope factor was reversed and the steeper *I–V* curve that facilitated channel activation at membrane potential above -57 mV generated the strongest burst firing (number of AP: $k = 2$: 8.4 ± 0.7, $k = 6$: 7.2 ± 0.7, $k = 10$: 6.5 ± 0.7, $P > 0.05$, $n = 7$; Fig. 5*Ac*). Accordingly, in the presence of the I_h blocker ZD7288, the slow repolarization that depends on T-channel recruitment was restored and the rebound excitability was similar to the one observed using short hyperpolarization of moderate amplitude (latency: $k = 2$: 101.0 ± 23.5 ms, $k = 6$: 48.5 ± 7.1 ms, $k = 10$: 29.8 ± 2.5 ms, $P \leq 0.05$, percentage of inactivated channels: $k = 2$: 82.9 ± 4.6, $k = 6$: 46.9 ± 3.3, $k = 10$: 28.4 ± 0.9, $P \leq 0.005$, number of AP: $k = 2$: 2.0 ± 0.8, $k = 6$: 7.5 ± 0.5, $k = 10$: 8.2 ± 0.5, $P \leq 0.001$, $n = 5$; Fig. 5*Ad*).

This tight link between the condition of LTS generation and the ability to trigger a burst suggests that not only the biophysical properties of the T current but also the triggering events need to be considered when assessing the physiological impact of T current activation. The two main excitatory pathways that converge on TC neurons, i.e. the sensory and corticothalamic afferents, generate very different glutamatergic EPSPs (Turner & Salt, 1998). As already shown in Figs 3 and 4, minimal stimulation of the internal capsule to activate the corticothalamic fibres elicited typical corticothalamic EPSPs of small amplitude which are characterized by a slow rising phase and a robust frequency-dependent facilitation. In contrast, single minimal stimulation of the sensory lemniscal pathway evoked a large-amplitude and fast rising EPSP. As a consequence, and consistent with the mechanism described above, slight modifications of the activation slope (Fig. 5*Ba*) produced opposite effects depending on whether the bursts were generated by corticothalamic or lemniscal EPSPs (Fig. 5*Bb*). Because the slow depolarization that occurs during corticothalamic EPSPs was significantly accelerated by IT_a activation at hyperpolarized potentials, the shallowest activation slope allowed the largest T channel recruitment at potentials between -80 and -57 mV and shortened the depolarization phase leading to minimal T channel inactivation and subsequently large LTS generation associated with the strongest burst firing (Fig. 5*Bb*, Table 1). Conversely, the LTS threshold was readily crossed by lemniscal EPSP and T channel inactivation did not occur before LTS generation. Therefore, IT_a with the steepest slope that facilitates channel activation for membrane potentials above -57 mV generated the strongest burst (Fig. 5*Bb*, Table 1).

Close monitoring of the injected dynamic-clamp current and the gating states of the model was also performed during GABAergic IPSPs. As shown in Fig. 6*A* and *B*, IT_a with a shallow activation slope ($k = 8$) was already activated during the train of IPSPs. As IT_a activation counteracts the synaptic hyperpolarization, the membrane potential was more depolarized than in control condition ($k = 6$) at the end of the IPSP train. Therefore, fewer channels could recover from inactivation during the train of IPSPs inducing a reduction in IT_a amplitude during the LTS and a smaller burst generation than that observed when a control IT_a was injected. In contrast, the level of hyperpolarization reached during the bursts of IPSPs was identical for *k* values of 4 and 6. However, during the repolarization, control IT_a ($k = 6$) was activated earlier than IT_a with the steepest activation slope ($k = 4$). As a

and generate a rebound LTS. Note that the initial repolarization phase is delayed with the slope factor 2 that does not allow significant recruitment of T channels at membrane potentials more negative than -57 mV. Monitoring of the percentage of inactivation (1-h) indicates that a significantly larger inactivation of T channels occurs when the initial repolarization is longer. Conversely, monitoring the activation (m, bottom line) indicates that the fastest initial repolarization occurred with the largest activation of T channels at hyperpolarized potential. *c*, LTSs (top traces) are evoked at the end of a 1 s hyperpolarization to -100 mV in a TC neuron from Cav3.1$^{-/-}$ mice in the presence of IT_a (middle traces) with the same slope factors as in *b*. Note that the fast repolarization kinetics are independent of the activation slope factor leading to minimal T channel inactivation (1-h,) prior to LTS generation. Note also that the largest bursts are observed with the steepest slope factor ($k = 2$). *d*, same protocols as in *c* in the presence of 50 μM ZD7288. Note that similarly to what was observed in *b*, the initial repolarization is delayed with the steepest activation curve allowing a large inactivation of T channels ($k = 2$). *B*, from a holding potential of -80 mV, LTSs are evoked by either a train of corticothalamic EPSPs (4 stimuli at 100 Hz, top records), or a single lemniscal EPSP (bottom records) in a TC neuron from Cav3.1$^{-/-}$ mice in the presence of IT_a with activation slope factor *k* equal to 4, 6 and 8. Note that maximal excitability is observed with the shallower ($k = 8$) activation curve for corticothalamic EPSPs (same example as in Fig. 4*Bd*) while the reverse is observed when LTS is triggered by the strong depolarization due to the lemniscal input.

consequence, for $k = 4$, the first phase of repolarization was delayed and T channel inactivation occurred, leading once again to smaller burst generation than with control IT_a.

Discussion

This study provides the first direct demonstration that (i) in both TC and NRT neurons the characteristic high-frequency burst firing pattern associated with LTSs closely depends on their T current kinetics; (ii) Ca^{2+} entry plays nearly no role in shaping the LTS-mediated burst firing of TC neurons; (iii) minimal modifications in the biophysical properties of the T current, especially in the voltage range corresponding to the foot of its *I–V* curve, drastically condition neuronal responses to synaptic potentials; (iv) these effects are highly dependent on the shape of the triggering event and hence are synaptic input specific. Altogether, our data illustrate that the dynamic-clamp technique combined with either pharmacological or genetic ablation of native T channels is an invaluable tool to dissect the physiological role of the T current and its associated Ca^{2+} entry in respect to the other intrinsic currents and synaptic input of a given neuron.

Despite the large number of studies on the role of LTSs in thalamic physiology (Llinas & Steriade, 2006), fundamental questions, such as the respective roles of depolarization and Ca^{2+} entry associated with T channel activation or the impact of T current gating on burst firing dynamics of TC neurons, have never been directly investigated experimentally. In particular, although both SK and BK channels are expressed in TC neurons (Stocker & Pedarzani, 2000; Sailer *et al.* 2004; Sausbier *et al.* 2006), the contribution of Ca^{2+}-activated K^+ currents to LTS has never been systematically analysed though a lack of effect of apamin on their burst firing has been reported (Kleiman-Weiner *et al.* 2009). In our experiments, however, the finer control of the T channel state and thus the higher reproducibility of the LTSs and associated bursts which were achieved by the use of the voltage-clamp mode during conditioning prepulses show no effect of a selective BK blocker on burst firing and a small but significant contribution of

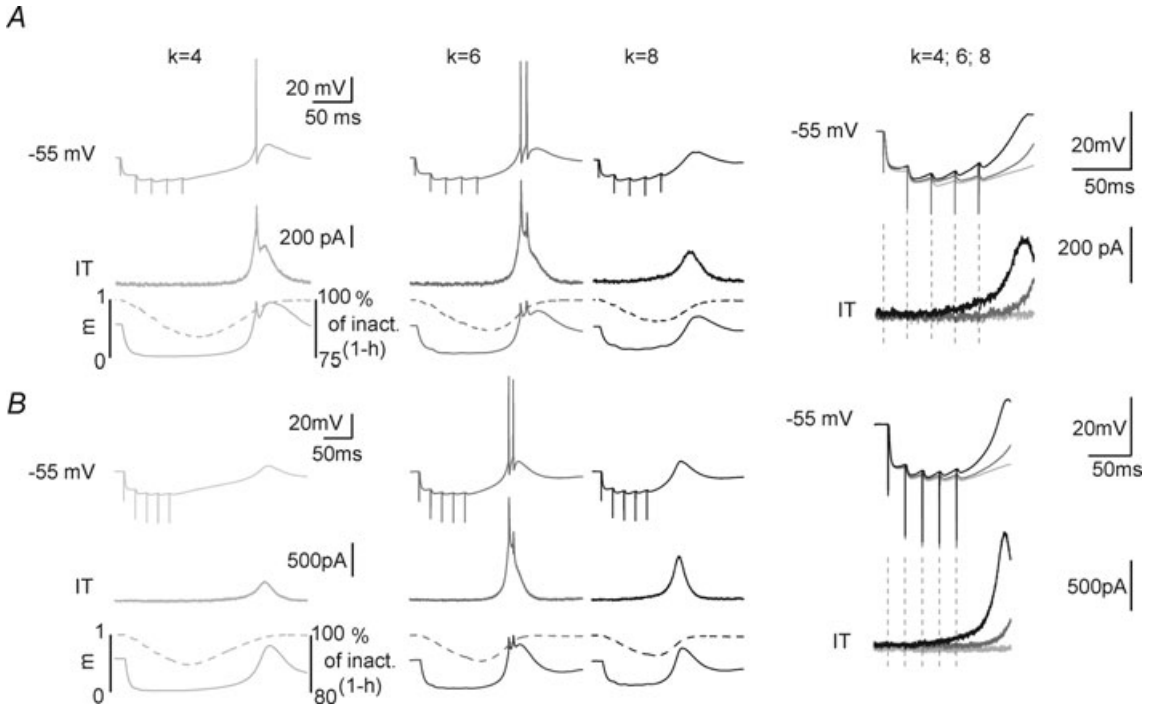

Figure 6. In TC neurons synaptically mediated LTS-rebound activity is conditioned by the base of the activation curve
Top traces in *A* and *B* show typical responses of 2 TC neurons from Cav3.1$^{-/-}$ mice submitted to a train of GABAergic IPSPs (5 stimuli at 50 Hz, holding potential = −55 mV) while injecting IT_a (middle traces) with activation slope factor 4, 6 and 10. Dynamics of activation (m, plain line) and inactivation (1-h, dotted line) gating during the protocol are shown in the bottom traces. Enlargement of the voltage traces and injected currents recorded during IPSPs and membrane repolarization are superimposed on the right. Note that the maximal excitability is obtained with the control slope factor $k = 6$ (top traces). Note also that for the steeper activation curve ($k = 4$), almost no IT_a is injected at the end of the GABAergic train inducing a delayed repolarization and significant T channel inactivation. By contrast, for the shallower activation curve ($k = 8$), T channel activation already occurs during the train of IPSPs and reduces the hyperpolarization leading to a decreased recovery from inactivation.

SK channels to the LTS repolarization in TC neurons. Importantly, the latter had a marginal impact on neuronal firing since it added only one AP to the burst in 70% of the cells without changes in burst frequency. In addition, since injection of the IT_a that mimicked the T current-mediated depolarization fully restored the high-frequency burst in the absence of Ca^{2+} entry, activation of other Ca^{2+} sensitive conductances, e.g. non-selective cation currents (Williams *et al.* 1997), is unlikely to significantly participate in the burst firing of TC neurons, in contrast to lateral geniculate interneurones (Zhu *et al.* 1999) and NRT neurons (Bal & McCormick, 1993).

Therefore, since Ca^{2+} activated conductances have a negligible effect on the LTS high-frequency firing, TC neurons appear to be a privileged model for studying the physiological impact of changes in T current biophysical properties using dynamic-clamp. An important conclusion arising from our experiments is that T currents not only allow high-frequency firing during a burst but also shape the precise firing patterns of thalamic neurons by their gating dynamics.

This was first suggested by the presence of an accelerando-decelerando AP pattern within bursts recorded in TC neurons injected with IT_a-NRT, instead of their characteristic decelerando pattern. This clearly indicates that the biophysical characteristics of the T-type isoforms expressed in a neuronal type are the critical factors for defining the burst signature, as originally suggested by Huguenard & Prince (1992). Later modelling studies, however, proposed that the accelerando-decelerando pattern of NRT neurons also arises from the slowly increasing current load provided by a Ca^{2+} spike occurring in distal dendrites, and is therefore highly dependent on the distal dendritic localization of T channels (Destexhe *et al.* 1996). The somatic injection of IT_a used in our study did not allow us to confirm or invalidate this prediction. However, the presence of the native burst signature in NRT neurons somatically injected with IT_a-NRT together with its loss when IT_a-TC was introduced clearly suggests that the specific kinetics of the NRT Cav3.2 and 3.3 channels (Talley *et al.* 1999) are a key element to define the burst pattern.

Our systematic studies of the functional impact of T channel gating parameters in TC neurons demonstrated that very small modifications in the voltage dependence of both channel activation and inactivation drastically affect burst firing. The precise description of the impact of these changes may be partially hampered by the somatic localization of injected IT_a, a major limitation of the dynamic clamp technique. However, based upon previous work that experimentally investigated T channel localization in TC neurons, these channels are preferentially expressed in the first micrometres of proximal dendrites (Destexhe *et al.* 1998; Williams & Stuart, 2000), and thus the influence of the space effect should be minimal. In addition, a recent modelling study analysing the impact of dendritic T channel localization has demonstrated that if the number of T channels has a prime influence on LTS bursting, their exact localization becomes important only in a very limited range of the total number of T channels (Zomorrodi *et al.* 2008). Using a similar approach, Rhodes & Llinas (2005) showed that although the fast high threshold Ca^{2+} events might occur in distal dendritic branches, the slower LTSs are primarily driven by T current located in the somatic and proximal dendritic membrane. Therefore, these data suggest that contrary to what has been shown for NRT neurons, distally localized T channels have no major impact on LTS generation in TC neurons. However, as highlighted by Destexhe & Sejnowski (2003) these dendritic T channels may locally interact with synaptic inputs affecting the integration properties of TC neurons. Currently, such complex interactions cannot be experimentally investigated and further modelling studies will be required to fully understand how small variations in T channel gating properties affect local synaptic integration.

To date the majority of reported T current modulations involve alterations in the channel biophysical properties (Chemin *et al.* 2001*c*; Iftinca *et al.* 2007; Traboulsie *et al.* 2007; Barbara *et al.* 2009; Hildebrand *et al.* 2009). These data have been mainly obtained in recombinant systems where the functional analysis is restricted to examination of the response characteristics of T channels under mock neuronal activities (Chemin *et al.* 2001*c*; Cataldi *et al.* 2007; Traboulsie *et al.* 2007). Such strategies provide limited information on the potential physiological consequences of these modulations since they do not take into account how the T current interacts with the other intrinsic membrane currents and the mock neuronal activity is not adjusted in real time with respect to the evoked T current. The variations in gating voltage dependence that were introduced in the T current model described here are well within the range of the reported modifications of T currents by endogenous ligands and/or intracellular pathways (Chemin *et al.* 2001*c*; Iftinca *et al.* 2007; Traboulsie *et al.* 2007; Barbara *et al.* 2009; Hildebrand *et al.* 2009; Park *et al.* 2010). Our results can therefore be extrapolated to predict the functional impact of T channel regulation in a physiological environment. Moreover, a critical appraisal of the literature indicates that some ligands/neurotransmitters which have been considered not to modulate T current properties do indeed produce changes in the channel gating that are well in the range of those studied here (see for example Fig. 1*d* in Iftinca *et al.* 2007). Therefore, subtle regulations of the T current that are at the limit of the resolution of classical biophysical studies may still have profound consequences on firing dynamics when neurons are challenged with synaptic stimuli, and some

physiologically significant T current regulations may have been neglected in these biophysical studies. In this respect, great attention should be directed to the channel properties in the voltage range corresponding to the foot of the *I–V* curves. In this voltage range, the steady-state inactivation and activation curves overlap defining a window current (Perez-Reyes, 2003) that has a profound implication for setting the resting membrane potential (Dreyfus *et al.* 2010) and controlling sleep-related oscillations (Hughes *et al.* 2002; Dreyfus *et al.* 2010). Here, we demonstrate for the first time that the channel activation and inactivation which occur concomitantly at these potentials also exert a complex control of synaptically induced burst firing. As a consequence, any modulation of these gating properties will modify the balance between the fraction of inactivated and closed channels at the moment of the LTS generation, changing in turn the temporal dynamics of firing. These effects are pronounced when LTSs are triggered in TC neurons by a train of IPSPs or weak EPSPs following activation of NRT and cortical inputs, respectively. However, because sensory EPSPs are fast-rising large synaptic events, the slow depolarizing phase preceding the LTS does not exist and because little T channel inactivation occurs before actual LTS generation, the sensory input is insensitive to variation occurring at the foot of the *I–V* curves. A similar dependence in burst generation and properties according to the nature of the synaptic inputs was previously reported by our group in the context of the up-regulation of the T current that occurs in sensory TC neurons at depolarized potentials (Leresche *et al.* 2004; Bessaih *et al.* 2008). This also emphasizes the importance of a contextual activation of the T current when studying its role in neuronal excitability.

Multiple splice variants that differ in kinetics and voltage dependence have been described for each T channel isoform (Chemin *et al.* 2001*a*,*b*; Murbartian *et al.* 2002, 2004; Latour *et al.* 2004; Emerick *et al.* 2006; Zhong *et al.* 2006; Powell *et al.* 2009). Some of these splice variants were shown to be expressed in the thalamus (Broicher *et al.* 2007; Ernst & Noebels, 2009; Powell *et al.* 2009, and see supplemental Fig. 3*A*), and a point mutation in Cav3.2 that segregates with seizure expression was reported to display splice variant-specific effects (Powell *et al.* 2009). Although the functional impact of the expression of these various splice variants is still conjectural, our data strongly suggest that the heterogeneity of the T current biophysical properties resulting from their expression should markedly affect thalamic neuron firing dynamics. Indeed, as shown in Supplemental Fig. 3, when an IT_a mimicking the human Cav3.1bc or Cav3.1be splice variants was introduced in TC neurons from Cav3.1$^{-/-}$ mice drastic differences in rebound burst firing triggered by a physiological-like hyperpolarization were observed, although these splice variants had been shown to display only very small differences in their biophysical properties (Chemin *et al.* 2001*a*).

In conclusion, even subtle modifications in the biophysical properties of the T current, either due to ligand mediated regulation or specific splice variant expression, are likely to drastically affect both the number and the temporal dynamics of APs in TC neuron bursts, and therefore condition information integration and transfer through the thalamus. Indeed, it has been elegantly demonstrated *in vivo* that putative LTS-associated APs in TC neurons are far more effective in eliciting postsynaptic action potentials in cortical neurons than tonic firing. This applies not only to the first AP of a burst but also to later APs which occur with a frequency >250 Hz (Swadlow & Gusev, 2001; Swadlow *et al.* 2005).

References

Avanzini G, de Curtis M, Panzica F & Spreafico R (1989). Intrinsic properties of nucleus reticularis thalami neurones of the rat studied *in vitro*. *J Physiol* **416**, 111–122.

Bal T & McCormick DA (1993). Mechanisms of oscillatory activity in guinea-pig nucleus reticularis thalami *in vitro*: a mammalian pacemaker. *J Physiol* **468**, 669–691.

Barbara G, Alloui A, Nargeot J, Lory P, Eschalier A, Bourinet E & Chemin J (2009). T-type calcium channel inhibition underlies the analgesic effects of the endogenous lipoamino acids. *J Neurosci* **29**, 13106–13114.

Bessaih T, Leresche N & Lambert RC (2008). T current potentiation increases the occurrence and temporal fidelity of synaptically evoked burst firing in sensory thalamic neurons. *Proc Natl Acad Sci U S A* **105**, 11376–11381.

Broicher T, Kanyshkova T, Landgraf P, Rankovic V, Meuth P, Meuth SG, Pape HC & Budde T (2007). Specific expression of low-voltage-activated calcium channel isoforms and splice variants in thalamic local circuit interneurons. *Mol Cell Neurosci* **36**, 132–145.

Cataldi M, Lariccia V, Marzaioli V, Cavaccini A, Curia G, Viggiano D, Canzoniero LM, di Renzo G, Avoli M & Annunziato L (2007). Zn^{2+} slows down $Ca_V3.3$ gating kinetics: implications for thalamocortical activity. *J Neurophysiol* **98**, 2274–2284.

Chemin J, Mezghrani A, Bidaud I, Dupasquier S, Marger F, Barrere C, Nargeot J & Lory P (2007). Temperature-dependent modulation of Ca_V3 T-type calcium channels by protein kinases C and A in mammalian cells. *J Biol Chem* **282**, 32710–32718.

Chemin J, Monteil A, Bourinet E, Nargeot J & Lory P (2001*a*). Alternatively spliced α_{1G} ($Ca_V3.1$) intracellular loops promote specific T-type Ca^{2+} channel gating properties. *Biophys J* **80**, 1238–1250.

Chemin J, Monteil A, Dubel S, Nargeot J & Lory P (2001*b*). The α_{1I} T-type calcium channel exhibits faster gating properties when overexpressed in neuroblastoma/glioma NG 108-15 cells. *Eur J Neurosci* **14**, 1678–1686.

Chemin J, Monteil A, Perez-Reyes E, Nargeot J & Lory P (2001*c*). Direct inhibition of T-type calcium channels by the endogenous cannabinoid anandamide. *EMBO J* **20**, 7033–7040.

Coulter DA, Huguenard JR & Prince DA (1989). Calcium currents in rat thalamocortical relay neurones: kinetic properties of the transient, low-threshold current. *J Physiol* **414**, 587–604.

Crunelli V, Lightowler S & Pollard CE (1989). A T-type Ca^{2+} current underlies low-threshold Ca^{2+} potentials in cells of the cat and rat lateral geniculate nucleus. *J Physiol* **413**, 543–561.

Destexhe A, Contreras D, Steriade M, Sejnowski TJ & Huguenard JR (1996). In vivo, in vitro, and computational analysis of dendritic calcium currents in thalamic reticular neurons. *J Neurosci* **16**, 169–185.

Destexhe A, Neubig M, Ulrich D & Huguenard J (1998). Dendritic low-threshold calcium currents in thalamic relay cells. *J Neurosci* **18**, 3574–3588.

Destexhe A & Sejnowski TJ (2003). Interactions between membrane conductances underlying thalamocortical slow-wave oscillations. *Physiol Rev* **83**, 1401–1453.

Domich L, Oakson G & Steriade M (1986). Thalamic burst patterns in the naturally sleeping cat: a comparison between cortically projecting and reticularis neurones. *J Physiol* **379**, 429–449.

Dreyfus FM, Tscherter A, Errington AC, Renger JJ, Shin HS, Uebele VN, Crunelli V, Lambert RC & Leresche N (2010). Selective T-type calcium channel block in thalamic neurons reveals channel redundancy and physiological impact of $I_T$window. *J Neurosci* **30**, 99–109.

Emerick MC, Stein R, Kunze R, McNulty MM, Regan MR, Hanck DA & Agnew WS (2006). Profiling the array of $Ca_v3.1$ variants from the human T-type calcium channel gene CACNA1G: alternative structures, developmental expression, and biophysical variations. *Proteins* **64**, 320–342.

Ernst WL & Noebels JL (2009). Expanded alternative splice isoform profiling of the mouse Cav3.1/α1G T-type calcium channel. *BMC Mol Biol* **10**, 53.

Hildebrand ME, Isope P, Miyazaki T, Nakaya T, Garcia E, Feltz A, Schneider T, Hescheler J, Kano M, Sakimura K, Watanabe M, Dieudonne S & Snutch TP (2009). Functional coupling between mGluR1 and Cav3.1 T-type calcium channels contributes to parallel fiber-induced fast calcium signaling within Purkinje cell dendritic spines. *J Neurosci* **29**, 9668–9682.

Hughes SW, Cope DW, Blethyn KL & Crunelli V (2002). Cellular mechanisms of the slow (1 Hz) oscillation in thalamocortical neurons in vitro. *Neuron* **33**, 947–958.

Huguenard JR & McCormick DA (1992). Simulation of the currents involved in rhythmic oscillations in thalamic relay neurons. *J Neurophysiol* **68**, 1373–1383.

Huguenard JR & Prince DA (1992). A novel T-type current underlies prolonged Ca^{2+}-dependent burst firing in GABAergic neurons of rat thalamic reticular nucleus. *J Neurosci* **12**, 3804–3817.

Iftinca M, Hamid J, Chen L, Varela D, Tadayonnejad R, Altier C, Turner RW & Zamponi GW (2007). Regulation of T-type calcium channels by Rho-associated kinase. *Nat Neurosci* **10**, 854–860.

Jahnsen H & Llinas R (1984). Electrophysiological properties of guinea-pig thalamic neurones: an *in vitro* study. *J Physiol* **349**, 205–226.

Kim D, Song I, Keum S, Lee T, Jeong MJ, Kim SS, McEnery MW & Shin HS (2001). Lack of the burst firing of thalamocortical relay neurons and resistance to absence seizures in mice lacking α_{1G} T-type Ca^{2+} channels. *Neuron* **31**, 35–45.

Kleiman-Weiner M, Beenhakker MP, Segal WA & Huguenard JR (2009). Synergistic roles of GABAA receptors and SK channels in regulating thalamocortical oscillations. *J Neurophysiol* **102**, 203–213.

Klockner U, Lee JH, Cribbs LL, Daud A, Hescheler J, Pereverzev A, Perez-Reyes E & Schneider T (1999). Comparison of the Ca^{2+} currents induced by expression of three cloned α1 subunits, α_{1G}, α_{1H} and α_{1I}, of low-voltage-activated T-type Ca^{2+} channels. *Eur J Neurosci* **11**, 4171–4178.

Kozlov AS, McKenna F, Lee JH, Cribbs LL, Perez-Reyes E, Feltz A & Lambert RC (1999). Distinct kinetics of cloned T-type Ca^{2+} channels lead to differential Ca^{2+} entry and frequency-dependence during mock action potentials. *Eur J Neurosci* **11**, 4149–4158.

Lambert RC, Bessaih T & Leresche N (2006). Modulation of neuronal T-type calcium channels. *CNS Neurol Disord Drug Targets* **5**, 611–627.

Latour I, Louw DF, Beedle AM, Hamid J, Sutherland GR & Zamponi GW (2004). Expression of T-type calcium channel splice variants in human glioma. *Glia* **48**, 112–119.

Leresche N, Hering J & Lambert RC (2004). Paradoxical potentiation of neuronal T-type Ca^{2+} current by ATP at resting membrane potential. *J Neurosci* **24**, 5592–5602.

Lisman JE (1997). Bursts as a unit of neural information: making unreliable synapses reliable. *Trends Neurosci* **20**, 38–43.

Llinas R & Jahnsen H (1982). Electrophysiology of mammalian thalamic neurones in vitro. *Nature* **297**, 406–408.

Llinas R & Muhlethaler M (1988). Electrophysiology of guinea-pig cerebellar nuclear cells in the *in vitro* brain stem–cerebellar preparation. *J Physiol* **404**, 241–258.

Llinas R & Yarom Y (1981). Electrophysiology of mammalian inferior olivary neurones in vitro. Different types of voltage-dependent ionic conductances. *J Physiol* **315**, 549–567.

Llinas RR & Steriade M (2006). Bursting of thalamic neurons and states of vigilance. *J Neurophysiol* **95**, 3297–3308.

Monteil A, Chemin J, Bourinet E, Mennessier G, Lory P & Nargeot J (2000*a*). Molecular and functional properties of the human α_{1G} subunit that forms T-type calcium channels. *J Biol Chem* **275**, 6090–6100.

Monteil A, Chemin J, Leuranguer V, Altier C, Mennessier G, Bourinet E, Lory P & Nargeot J (2000*b*). Specific properties of T-type calcium channels generated by the human α_{1I} subunit. *J Biol Chem* **275**, 16530–16535.

Murbartian J, Arias JM, Lee JH, Gomora JC & Perez-Reyes E (2002). Alternative splicing of the rat $Ca_v3.3$ T-type calcium channel gene produces variants with distinct functional properties. *FEBS Lett* **528**, 272–278.

Murbartian J, Arias JM & Perez-Reyes E (2004). Functional impact of alternative splicing of human T-type Cav3.3 calcium channels. *J Neurophysiol* **92**, 3399–3407.

Nelson MT, Joksovic PM, Perez-Reyes E & Todorovic SM (2005). The endogenous redox agent L-cysteine induces T-type Ca^{2+} channel-dependent sensitization of a novel subpopulation of rat peripheral nociceptors. *J Neurosci* **25**, 8766–8775.

Park YG, Park HY, Lee CJ, Choi S, Jo S, Choi H, Kim YH, Shin HS, Llinas RR & Kim D (2010). $Ca_V3.1$ is a tremor rhythm pacemaker in the inferior olive. *Proc Natl Acad Sci U S A* **107**, 10731–10736.

Perez-Reyes E (2003). Molecular physiology of low-voltage-activated T-type calcium channels. *Physiol Rev* **83**, 117–161.

Powell KL, Cain SM, Ng C, Sirdesai S, David LS, Kyi M, Garcia E, Tyson JR, Reid CA, Bahlo M, Foote SJ, Snutch TP & O'Brien TJ (2009). A Cav3.2 T-type calcium channel point mutation has splice-variant-specific effects on function and segregates with seizure expression in a polygenic rat model of absence epilepsy. *J Neurosci* **29**, 371–380.

Rhodes PA & Llinas R (2005). A model of thalamocortical relay cells. *J Physiol* **565**, 765–781.

Sailer CA, Kaufmann WA, Marksteiner J & Knaus HG (2004). Comparative immunohistochemical distribution of three small-conductance Ca^{2+}-activated potassium channel subunits, SK1, SK2, and SK3 in mouse brain. *Mol Cell Neurosci* **26**, 458–469.

Sausbier U, Sausbier M, Sailer CA, Arntz C, Knaus HG, Neuhuber W & Ruth P (2006). Ca^{2+}-activated K^+ channels of the BK-type in the mouse brain. *Histochem Cell Biol* **125**, 725–741.

Shipe WD, Barrow JC, Yang ZQ, Lindsley CW, Yang FV, Schlegel KA, Shu Y, Rittle KE, Bock MG, Hartman GD, Tang C, Ballard JE, Kuo Y, Adarayan ED, Prueksaritanont T, Zrada MM, Uebele VN, Nuss CE, Connolly TM, Doran SM, Fox SV, Kraus RL, Marino MJ, Graufelds VK, Vargas HM, Bunting PB, Hasbun-Manning M, Evans RM, Koblan KS & Renger JJ (2008). Design, synthesis, and evaluation of a novel 4-aminomethyl-4-fluoropiperidine as a T-type Ca^{2+} channel antagonist. *J Med Chem* **51**, 3692–3695.

Stocker M & Pedarzani P (2000). Differential distribution of three Ca^{2+}-activated K^+ channel subunits, SK1, SK2, and SK3, in the adult rat central nervous system. *Mol Cell Neurosci* **15**, 476–493.

Swadlow HA, Bezdudnaya T & Gusev AG (2005). Spike timing and synaptic dynamics at the awake thalamocortical synapse. *Prog Brain Res* **149**, 91–105.

Swadlow HA & Gusev AG (2001). The impact of 'bursting' thalamic impulses at a neocortical synapse. *Nat Neurosci* **4**, 402–408.

Talley EM, Cribbs LL, Lee JH, Daud A, Perez-Reyes E & Bayliss DA (1999). Differential distribution of three members of a gene family encoding low voltage-activated (T-type) calcium channels. *J Neurosci* **19**, 1895–1911.

Traboulsie A, Chemin J, Chevalier M, Quignard JF, Nargeot J & Lory P (2007). Subunit-specific modulation of T-type calcium channels by zinc. *J Physiol* **578**, 159–171.

Turner JP & Salt TE (1998). Characterization of sensory and corticothalamic excitatory inputs to rat thalamocortical neurones *in vitro*. *J Physiol* **510**, 829–843.

Williams SR & Stuart GJ (2000). Action potential backpropagation and somato-dendritic distribution of ion channels in thalamocortical neurons. *J Neurosci* **20**, 1307–1317.

Williams SR, Toth TI, Turner JP, Hughes SW & Crunelli V (1997). The 'window' component of the low threshold Ca^{2+} current produces input signal amplification and bistability in cat and rat thalamocortical neurones. *J Physiol* **505**, 689–705.

Wolfart J, Debay D, Le Masson G, Destexhe A & Bal T (2005). Synaptic background activity controls spike transfer from thalamus to cortex. *Nat Neurosci* **8**, 1760–1767.

Zhong X, Liu JR, Kyle JW, Hanck DA & Agnew WS (2006). A profile of alternative RNA splicing and transcript variation of CACNA1H, a human T-channel gene candidate for idiopathic generalized epilepsies. *Hum Mol Genet* **15**, 1497–1512.

Zhu JJ, Uhlrich DJ & Lytton WW (1999). Burst firing in identified rat geniculate interneurons. *Neuroscience* **91**, 1445–1460.

Zomorrodi R, Kroger H & Timofeev I (2008). Modeling thalamocortical cell: impact of Ca channel distribution and cell geometry on firing pattern. *Front Comput Neurosci* **2**, 5.

Author contributions

A.T., F.D., T.I., T.B., C.D., N.L. and R.C.L. contributed to data collection and analysis. A.T., N.L. and R.C.L. contributed to the conception and design of experiments, the drafting of the article as well as revising it critically for important intellectual content. V.N.U. and J.J.R. provided the TTA-P2, H.S.S. the initial pair of Cav3.1KO mice. All authors have approved the final version of the manuscript.

Acknowledgements

This work was supported by the ANR-06-Neuro. Conflict of interest: J.J.R. and V.N.U. are employees of Merck and Co., Inc. (USA) and potentially own stock and/or stock options in the company.